

# Field and Laboratory Evaluation of the Mechanical Behavior of Unbound Granular Materials in Pavements

M. A. KAMAL, A. R. DAWSON, O. T. FAROUKI, D. A. B. HUGHES, AND  
A. A. SHA'AT

Laboratory and full-scale pavement studies were conducted as a part of an overall program to evaluate the engineering properties and performance of eight gradings of unbound granular roadbase materials. A repeated load triaxial testing program was conducted in conjunction with shear box and permeability tests on unbound mixes with grading curves ranging between the two extremes of the envelope currently used as a specification in the United Kingdom. After analyzing the laboratory results, full-scale trials were conducted using eight experimental gradings. The pavement test strip was divided into eight 22-m bays. Dynamic cone penetrometer, density, and moisture content measurements were performed on the subgrade, capping layer, and roadbase material. The performance of each bay under heavy traffic was monitored for 6 months. The rut depth profile was recorded using an automatic computerized rut profiler, and deflection measurements were recorded weekly by the deflectograph. Falling weight deflectometer testing was conducted three times. The objective of the research was to identify a material that would allow free drainage and hence reduce pumping and excess pore water pressure but maintain a high in situ stiffness with good resistance to permanent deformation.

The triaxial test is commonly used to assess the resilient modulus of unbound granular materials. The effect of aggregate grading was studied by Shaw (1). A comparison was made between 40-mm maximum-size broadly graded crushed rock roadbase material and a 3-mm single-sized stone from the same source. The broadly graded material was found to be much stiffer than the single-size stone, partly due to the large difference in maximum particle size. Thom (2) conducted a series of repeated load tests on 10-mm maximum-sized crushed dolomitic limestone and found a high stiffness for uniformly graded materials, but broadly graded material showed a higher shear strength. Thompson and Smith, however (3), reported that permanent deformation under repeated loading provides a more definitive evaluation of granular base materials than does resilient modulus or shear strength.

M. A. Kamal, O. T. Farouki, and D. A. B. Hughes, Civil Engineering Department, The Queen's University of Belfast, Stranmillis Road, Belfast, BT9 5AG Northern Ireland. A. R. Dawson, Civil Engineering Department, University of Nottingham, University Park, Nottingham, NG7 2RQ England. A. A. Sha'at, Civil Engineering Department, Dundee Institute of Technology, Dundee, Scotland.

## SAMPLE PREPARATION, APPARATUS, AND TEST ROUTINE

A large sample of aggregates obtained from a local gritstone quarry was air dried and separated into 10 single-sized fractions from which 10 mixes and 2 gradings at the extreme ends of the current United Kingdom specification (4) of unbound roadbase material were prepared by mixing appropriate weights of each fraction. The following equation proposed by Cooper et al. (5) was used to select the new gradings:

$$P = \frac{(100 - F)(d^n - 0.075^n)}{(D^n - 0.075^n)} + F$$

where

$P$  = percentage passing a sieve of size  $d$  mm,

$D$  = maximum particle size (mm),

$F$  = percentage of material passing through a 0.075 mm sieve, and

$n$  = increment in 0.1 steps.

This formula was selected because it maintains the fines content (i.e., passing through a 0.075-mm sieve) at a predetermined level, enabling the effective fines content (i.e., percentage of material passing through a 5-mm sieve) to be varied by adjusting the value of  $n$ . Some of the selected gradings are shown in Figure 1.

A specimen that was 150 mm in diameter and 300 mm long was tested in a repeated load triaxial facility developed by Boyce (6) at Nottingham. Six representative gradings were chosen in such a way as to cover a full range of mixes, that is, mixes 1, 3, 4, 6, 8, and 10 [see Figure 1(a)] along with the extreme ends of the current specification represented by gradings A and B in Figure 1(b). All specimens were identically prepared to achieve a dry density in the range of 1,950 to 2,170 kg/m<sup>3</sup> typical of field densities (see Full-Scale Trials in this paper). Specimens were compacted in five layers in a four-section split steel mould lined with a neoprene membrane. Each layer was compacted for 60 sec using a vibrating table and small surcharge, enabling the density to be controlled. Axial and radial strain measurements were taken by attaching linear variable differential transformers (LVDTs) and strain hoops to studs embedded in the sides of each specimen as shown in Figure 2. The apparatus was controlled by and the data were collected to a personal computer and high-

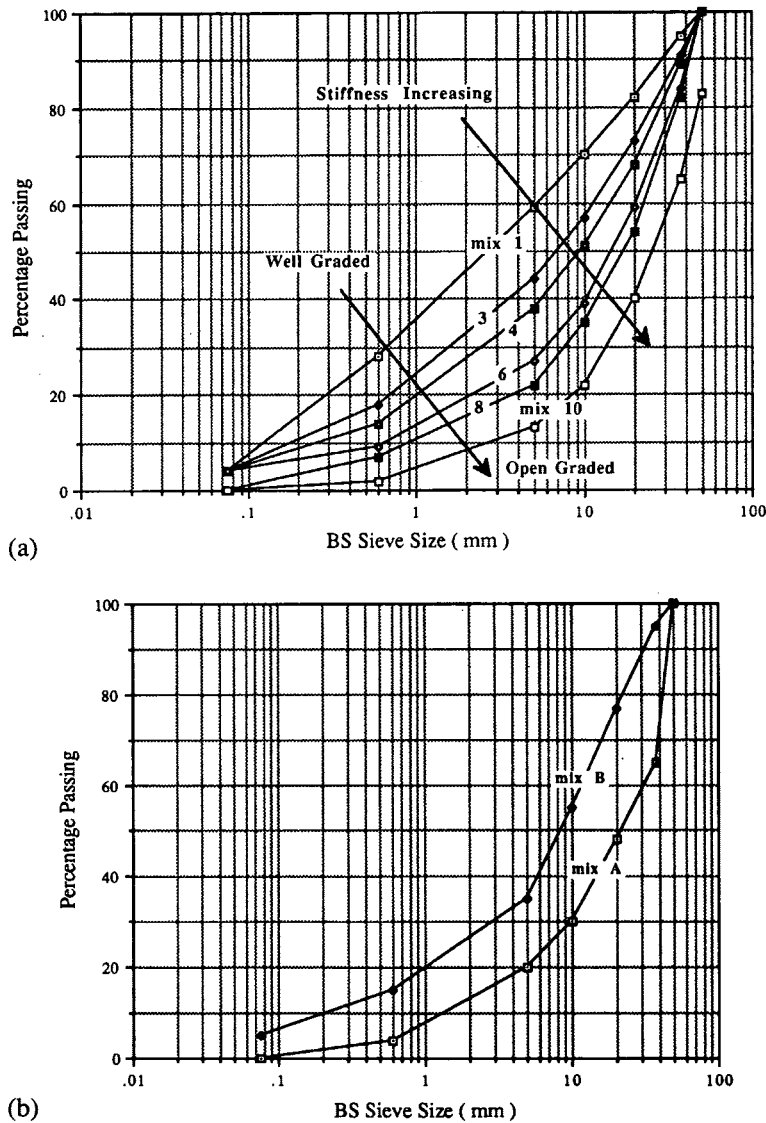


FIGURE 1 Selected gradings: (a) gradings used for triaxial and field testing and (b) extreme limits of current specifications (Mixes A and B).

speed digital/analogue control and acquisition hardware. The testing conducted on each specimen is described next.

First, to eliminate any seating problems between the load platens and the specimen, and to account for the initial traffic compaction experienced in field conditions, the load on each sample was repeatedly applied for 25,000 cycles at a deviator stress from 0 to 100 kPa, a confining pressure of 35 kPa, and a frequency of 5 Hz, allowing the plastic strain to develop before performing the repeated load elastic testing. The 25,000 cycles cause some bedding down and may represent long-term effects.

Second, repeated load elastic testing at a frequency of 1 Hz was performed along stress paths defined in terms of  $p$  and  $q$ , where  $p$  is the mean normal stress and  $q$  the deviator stress. The paths applied are presented in Table 1. All samples were tested at the dry end; therefore it is expected that changes in

$p$  accurately reflect the changes in  $p'$  (the mean normal effective stress). However, suctions were not measured, so the absolute value of  $p'$  is unknown.

Third, each sample was subjected to a repeated load plastic testing program as described in Step 1 for 10,000 cycles.

Finally, a failure test was performed at a constant confining stress of 35 kPa by increasing the deviator stress until the sample failed.

Mixes 1, 4, 6, 8, A, and B were subjected to stress paths from 1 to 28 (Table 1), whereas only stress paths 1 to 14 were used for mixes 3 and 10. For each test, the applied stress, axial strain, radial strain, and Poisson's ratio were directly recorded in the computer. Using the analysis package, the resilient modulus, stress-strain relationship, and permanent strain behavior of the dry granular material were analyzed. The results are described next.

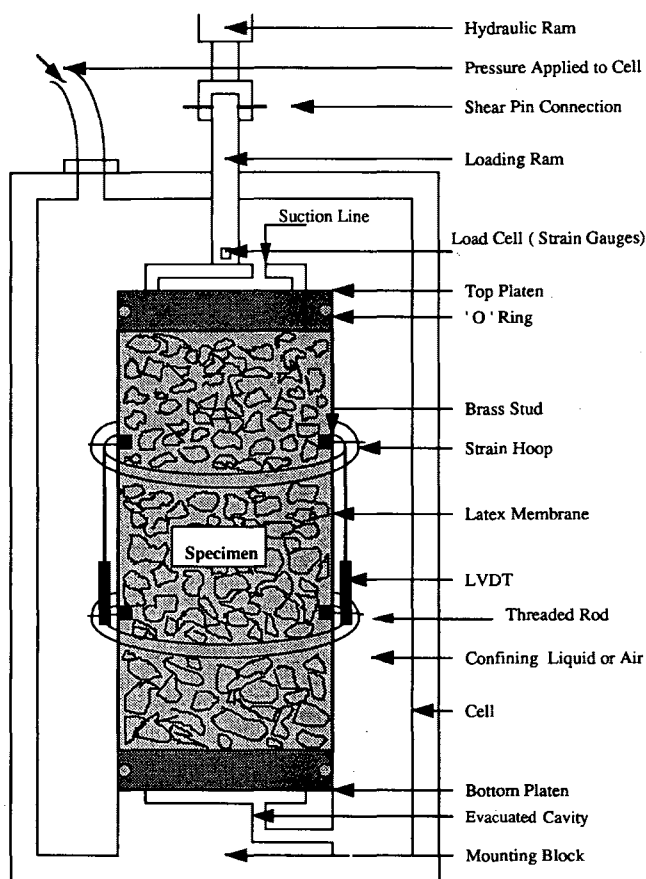


FIGURE 2 Triaxial cell arrangement.

## RESULTS

### Elastic Behavior

To analyze the results from the repeated load triaxial testing, the stress was expressed in terms of the sum of principal stresses ( $\theta = 3p = \sigma_1 + 2\sigma_3$ ) and the deviator stress ( $q = \sigma_1 - \sigma_3$ ). Resilient strain in a triaxial test has two components: resilient volumetric strain and resilient shear strain. For each mix, the resilient modulus ( $M_r$ ), shear strain ( $e_s$ ), and volumetric strain ( $e_v$ ) were calculated from the following relationships:

- Resilient modulus  $M_r = q/e_s$ ,
- Shear strain  $e_s = \frac{2}{3}(e_1 - e_3)$ , and
- Volumetric strain  $e_v = e_1 + 2e_3$ .

Suffixes 1 and 3 represent axial and radial directions, respectively.

### Resilient Modulus

For a direct comparison of the mixes at the same confining pressure when cycling from zero deviator stress, the resilient

TABLE 1 Stress Paths Used

Stress Path	q <sub>init</sub> (kPa)	q <sub>final</sub> (kPa)	p <sub>init</sub> (kPa)	p <sub>final</sub> (kPa)	$\sigma_3$ (kPa)	$\sigma_1$ init (kPa)	$\sigma_1$ final (kPa)
1	0	50	25	41.67	25	25	75
2	0	100	25	58.33	25	25	125
3	0	50	50	66.67	50	50	100
4	0	100	50	83.33	50	50	150
5	0	150	50	100	50	50	200
6	0	200	50	116.67	50	50	250
7	0	50	75	91.67	75	75	125
8	0	100	75	108.33	75	75	175
9	0	150	75	125	75	75	225
10	0	200	75	141.67	75	75	275
11	0	50	100	116.67	100	100	150
12	0	100	100	133.33	100	100	200
13	0	150	100	150	100	100	250
14	0	200	100	166.67	100	100	300
15	0	50	125	141.67	125	125	175
16	0	100	125	158.33	125	125	225
17	0	150	125	175	125	125	275
18	0	200	125	191.67	125	125	325
19	0	50	150	166.67	150	150	200
20	0	100	150	183.33	150	150	250
21	0	150	150	200	150	150	300
22	0	200	150	216.67	150	150	350
23	50	100	66.67	83.33	50	100	150
24	100	150	83.33	100	50	150	200
25	150	200	100	116.67	50	200	250
26	50	100	91.67	108.33	75	125	175
27	100	150	108.33	125	75	175	225
28	150	200	125	141.67	75	225	275

modulus of all the mixes was plotted against the sum of the principal stresses at 50 kPa confining pressure, as shown in Figure 3. It can be observed from Figure 3 that generally the resilient modulus increases from the finer to the coarser mix. It may also be seen that there is a slight increase in resilient modulus with increasing deviator stress. This latter effect is more noticeable at the higher values of stiffness.

An increase in resilient modulus was observed by increasing the confining pressure in the same manner for all the mixes for the stress paths 1 to 22 (shown in Table 1), that is, when cycling the deviator stress starting from zero. Stress Paths 23–25 start at nonzero values of deviator stress but end at the same stress levels as Paths 4–6, respectively; the repeated deviator stresses thus being smaller than for the earlier stress paths. For a higher confining pressure, Paths 26–28 may similarly be compared with Paths 8–10. Paths 3, 23, 24, and 25 may also be treated as a series of paths with the same repeated deviator stress, but at increasing levels of base deviator stress. The resilient moduli for Paths 23–28 are shown in Figure 4.

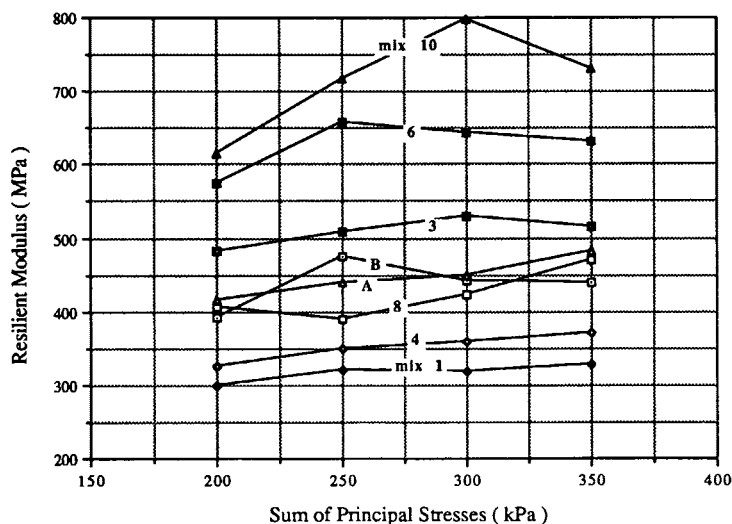


FIGURE 3 Resilient modulus of each mix at 50 kPa confining pressure (all mixes).

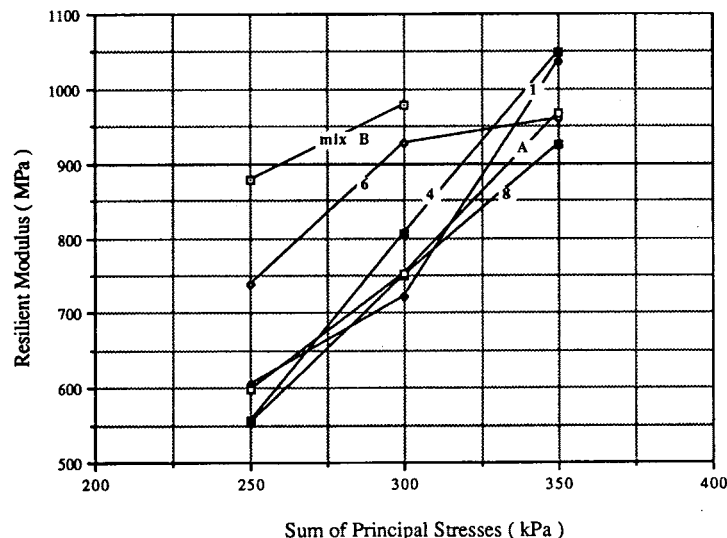


FIGURE 4 Resilient modulus of each mix at 50 kPa confining pressure (Paths 23-28).

By comparing Paths 4 and 23, 5 and 24, 6 and 25, 8 and 26, 9 and 27, and 10 and 28 (Figures 3 and 4), it can be seen that the stiffness increases as the base deviator stress rises, that is, the development of strain during a repeated load pulse varies during different parts of the pulse. This confirms the stress-dependent nature (i.e., nonlinearity) of the resilient modulus of unbound granular material. The same findings were reported by Lister and Jones (7) that unbound granular materials in a pavement usually have a markedly nonlinear stress-strain relationship and their effective modulus of elasticity increases with the increase of uniaxial pressure because of the increase in the contact area between adjacent grains.

#### Volumetric and Shear Strain

Volumetric strains are plotted against the natural logarithm of the stress ratio, that is,  $\ln(p_{final}/p_{init})$ , in Figure 5 for all the mixes at a confining pressure of 50 kPa. It can be seen that generally the volumetric strain decreases from the finer to the coarser mix. A decrease in volumetric strain with increasing confining pressure was also observed. The results show that the volumetric strain is directly affected by the presence of finer particles in the mixes, that is, it increases with increasing equivalent fines content, as discussed earlier. A similar trend with an increase in deviator stress and an

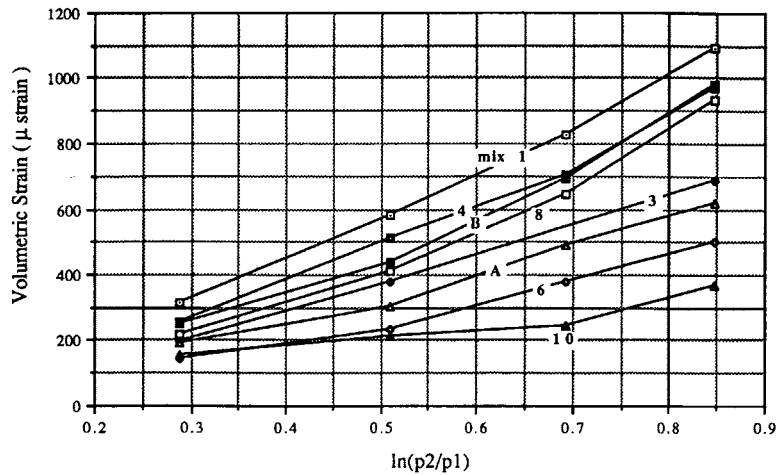


FIGURE 5 Volumetric strain versus  $\ln(p_2/p_1)$  for different mixes.

increase in mean normal stress was observed when the volumetric strain was plotted against the deviator stress and change in mean normal stress.

The shear strains are directly affected by the shear stress ratio ( $q/p$ ) (8) and therefore shear strains are plotted against change in shear stress ratio [ $\delta(q/p)$ ] for all the mixes at 50 kPa confining pressure, as shown in Figure 6. It can be seen from Figure 6 that the shear strain has the same trend as that of volumetric strain, that is, it decreases from the finer to the coarser mixes, indicating an increase in stiffness in the mix from the finer to the coarser end of the envelope. A decrease in shear strain with increasing confining pressure was also observed.

**Plastic Behavior**

Plastic behavior of a material in a repeated load triaxial apparatus was observed by applying a repeated deviator stress to the specimen and measuring the buildup of nonrecoverable strain against the number of cycles applied before performing the elastic testing program. The results for the log of per-

manent strain versus the log of the number of load repetitions are plotted in Figure 7. It can be seen that the resistance to permanent deformation generally increases for well-graded materials as compared to that of open-graded materials.

Before failure tests were performed, all samples were again subjected to repeated load testing to compare the rate of buildup of nonrecoverable strain before and after elastic testing. Each sample was confined at a pressure of 35 kPa, and the deviator stress was cycled from 0 to 100 kPa at a frequency of 5 Hz. Permanent deformation was recorded throughout the test until 10,000 stress repetitions had been applied. All materials were found to be stable, and the rate of permanent strain was negligible compared with the earlier results before the elastic testing as shown in Figure 7. The results are in good agreement with work by Morgan (9), who showed that even for  $10^6$  cycles, the material had not reached steady behavior.

**Failure Tests**

Failure tests were conducted on mixes A, 1, 4, 6, 10, and 5-mm single-sized aggregate to compare the shear strength of

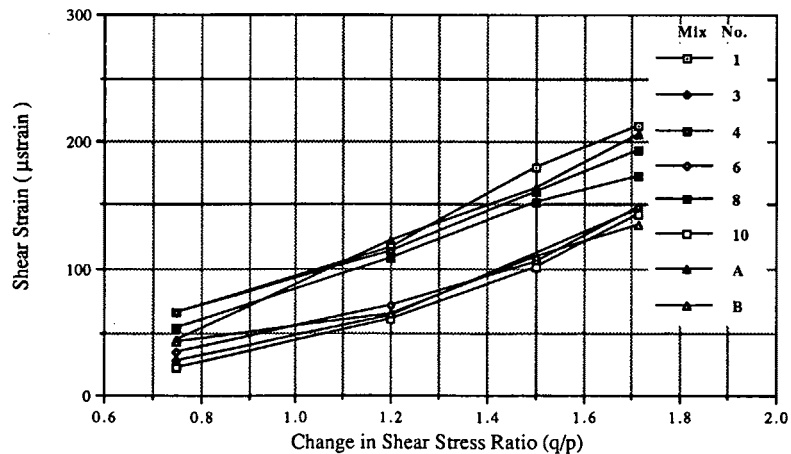
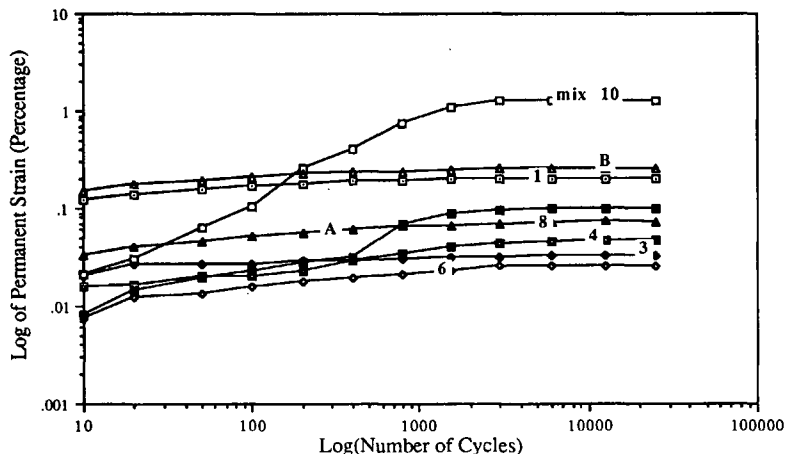


FIGURE 6 Shear strain versus change in shear stress ratio for each mix at 50 kPa confining pressure.



**FIGURE 7** Permanent strain versus number of cycles applied before resilient tests.

the materials. All the mixes were confined at a pressure of 35 kPa, and the deviator stress was increased from an initial value of zero until the specimen failed with a strain limit of 3 percent.

The principal stress ratio ( $\sigma_1/\sigma_3$ ) at failure relating to 35 kPa confining pressure was assumed as a simple strength indicator for a direct comparison of the designed mixes. The shear strength versus the principal stress ratio for the different mixes is shown in Figure 8. It can be seen that shear strength increased from the finer to the coarser side of the envelope. A similar trend was also observed when the shear stress ratio ( $q/p$ ) was assumed to be a failure measure.

**PERMEABILITY TEST**

Permeability tests were conducted on unbound granular material (10) on typical gritstone and basalt, ranging from well- to open-graded mixes, using the permeameter recommended

by the Department of Transport Highways and Traffic Advice Note (11). As a result of this investigation, the following permeability-grading relationship was proposed:

$$k = -69.2 - 22.1D_{10} + 24.7D_{20} + 228e + 6.96D_{10}^2 - 1.56D_{20}^2$$

where

- $k$  = permeability  $10^{-3}$  m/s,
- $D_{10}$  and  $D_{20}$  = effective sizes (mm) through which 10 percent and 20 percent material passes, respectively,
- $e$  = voids ratio of compacted sample with a value ranging from 0.26 to 0.58, and
- $R$  = correlation coefficient = 0.99.

The specific gravity of the aggregates was assumed to be 2.65.

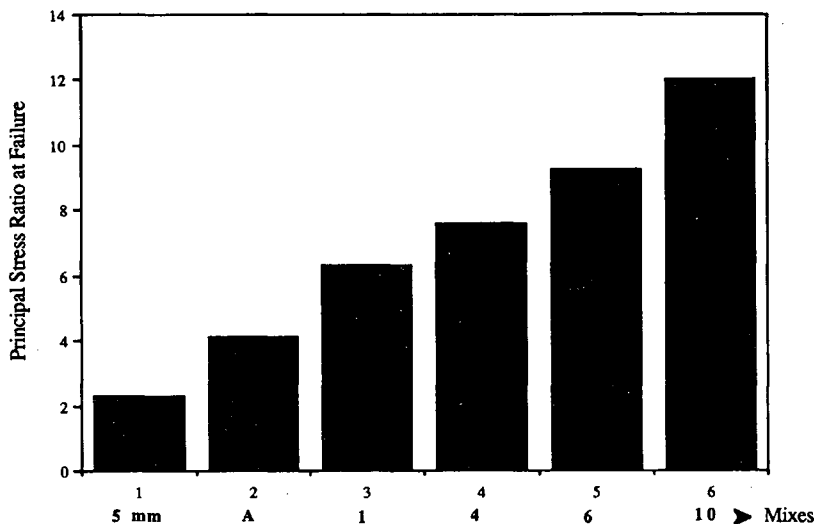


**FIGURE 8** Shear strength of different mixes at failure.

## FULL-SCALE TRIALS

Construction of the test strip started in July 1991, and the final surface was placed September 26, 1991. The test section at Dargan Road was located on an access point to a refuse disposal site. The test strip, 176 m long and 3.5 m wide, was excavated to a depth of about 700 mm to leave the finished surface of the test strip level with the existing pavement surface. A crusher run capping material with a maximum particle size of 75 mm was laid and compacted in two layers to provide a 350-mm thick layer and therefore a homogeneous platform for laying the proposed roadbase gradings. The test strip was divided into eight equal sections and the material was laid using a mechanical spreader and compacted using an 8-ton roller (five passes on both longitudinal ends) to achieve a 225-mm thick roadbase layer. Samples were collected during the laying process and brought to the laboratory for sieve analysis. The achieved gradings were found to be within 5 percent of the intended mixes. A 30-mm thick bituminous layer was laid on top of the roadbase to obtain a finished surface.

### In Situ Dynamic Cone Penetrometer (DCP), Moisture, and Density Measurements

DCP soundings were conducted on the subgrade, capping layer, and roadbase layer to assess the strength of each layer. At least three tests were performed in each bay. The California bearing ratio (CBR) values obtained using the DCP for the subgrade were analyzed on a personal computer using Kley's equation (12). The capping layer and roadbase were analyzed using the equation developed from laboratory testing of unbound granular material (13). The CBR values for the subgrade and capping layer were consistent (13 percent and 16 percent, respectively), showing that the subgrade and capping layer provided a homogeneous platform and allowed a realistic comparison of the behavior of the different bays.

In situ moisture contents and densities for the subgrade, capping layer, and roadbase were measured using a nuclear

density meter. The densities of the subgrade for the bays, with the exception of Bay 2, were in the range of 1,900 to 2,100 kg/m<sup>3</sup>. Bay 2 (Mix B) was 20 percent lower compared with the other bays. It was also observed that the subgrade moisture content of Bay 2 was about 50 percent higher than that for the other bays. The density and moisture content of the capping layer and the roadbase of all the bays were consistent. After construction, the number and loading of vehicles passing over the test section were assessed using a weigh bridge, and the data were used to convert the number of vehicles to equivalent standard axles.

### Falling Weight Deflectometer (FWD)

FWD and deflectograph tests were also conducted on the test strip. An average deflection and contact pressure for each bay was calculated to compare the different bays. Mix 1, which had a high effective fines content (percentage of material passing through a 5-mm sieve) with a coefficient of uniformity  $C_u$  (i.e.,  $D_{60}/D_{10}$ ) of 26, gave the maximum deflection. It was also observed that as  $C_u$  increased to a certain value, deflection reached a minimum, after which it started to increase. Therefore, the material with a greater percentage of effective fines content gave a higher deflection, and as the percentage of effective fines content decreased, the deflection also decreased to reach a minimum after which a further reduction in percentage of effective fines resulted in a higher deflection. This explains the minimum deflection achieved for both Mixes 4 and 6 with a  $C_u$  of 39 and 25, respectively. The mixes with lower effective fines content resulted in a more porous material, and the deflections were greater. There was an optimum percentage of effective fines, which gave a high density and good binding effect.

The values of the elastic modulus of the roadbase material for the different bays were analyzed using EVERCALC (14) and are shown in Figure 9. This figure shows that Mixes 4 and 6, with a  $C_u$  of 39 and 25, respectively, exhibited the greatest elastic moduli. The mixes on the finer side of the

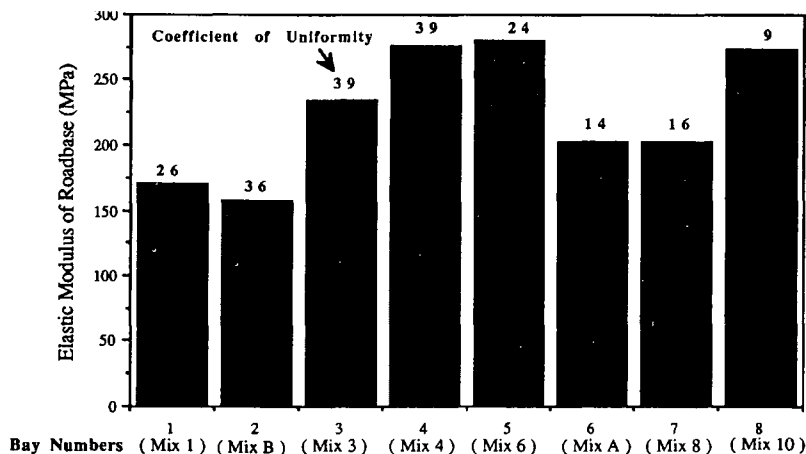


FIGURE 9 Elastic modulus for each roadbase material backcalculated from FWD measurements at Dargan Road.

envelope gave an increased number of possible contact points for movement within the mix to take place. This leads to a low value of elastic modulus as exhibited by Mix 1, which has a large percentage of effective fines. On the other hand, mixes on the coarser side of the other envelope with a smaller number of particles in a given volume showed higher elastic moduli.

### Deflectograph Testing

Deflection measurements were taken at the Dargan test strip fortnightly for 6 months with the British version of the deflectograph. For each bay, the representative value of the deflection bowl was computed and plotted against the number of standard axles passed in Figure 10. It was found that the deflection of all the bays was large before opening the test section to traffic. Densification occurred during the application of the first 2,500 standard axles. The observed deflections after this time were quite consistent in the respective bays. Mixes 4 and 6 showed the least deflection.

It was also observed that the materials having more than 40-percent effective fines showed a higher deflection. As the percentage of effective fines decreases and the coefficient of uniformity increases, the deflection decreases. A further reduction in effective fines produces a decrease in  $C_u$  and a more porous mix, resulting in an ultimate increase in deflection. This shows that the finer side of the proposed envelope (Figure 1) gives the higher deflection. The deflection decreases from the finer to the coarser side of the envelope up to a certain value, after which a further reduction in effective fines results in an increase in the deflection. This again shows that there is an optimum effective fines content. The anomalous behavior of Mix B could be due to the low density and higher moisture content for the subgrade in that bay as well as due to its low shear strength found in the laboratory. (For more details, refer to the section on DCP, moisture, and density measurements in this paper.)

### Automatic Rut Profiler

A realistic method for comparing the relative performance of the different proposed mixes is to measure the rut depth under actual vehicular loads and then compare the different designed mixes directly. As discussed previously, the subgrade, capping layer, and surfacing were the same for all the bays in the test strip. The only variable was the roadbase material. Therefore, the comparison of rut depth in the different bays provides a direct indication of the performance of the designed roadbase mixes. Rut depth was measured fortnightly using an automatic rut profiler.

The portable rut profiler consists of a 51-mm<sup>2</sup> steel beam with a recording box (175 mm × 120 mm) at one end. The three beams are fitted together for testing. The total length of the profiler is approximately 2.75 m. The beam sits on three large adjustable screws, and a steel trolley fitted with a flexible sensor (which sits on the surface of the pavement during the testing and records the rut) can slide on the beam. This instrument is used to plot the rut profile of the pavement; these data may be stored directly on a personal computer.

During this testing program, the rut profile of all the bays was measured in the transverse direction before opening the test section to traffic and was considered to be the baseline. Subsequently the rut measurements were conducted fortnightly. The transverse rut profiles for Mixes 6 and A are plotted against the standard axles passed in Figures 11 and 12 to show a comparison between the proposed (Mix 6) and current specifications (Mix A). The results showed that the base course in all the cases increased in thickness between the wheel paths, which is in good agreement with the findings of the AASHO Road Test (15). It was also observed in trials at Dargan Road that the depth of rut was more than twice as great for the open-graded material as for the well-graded ones. This shows that the resistance to permanent deformation decreases for the coarsely graded material as compared with the more well-graded materials. The same trend was observed from the repeated load plastic tests conducted in

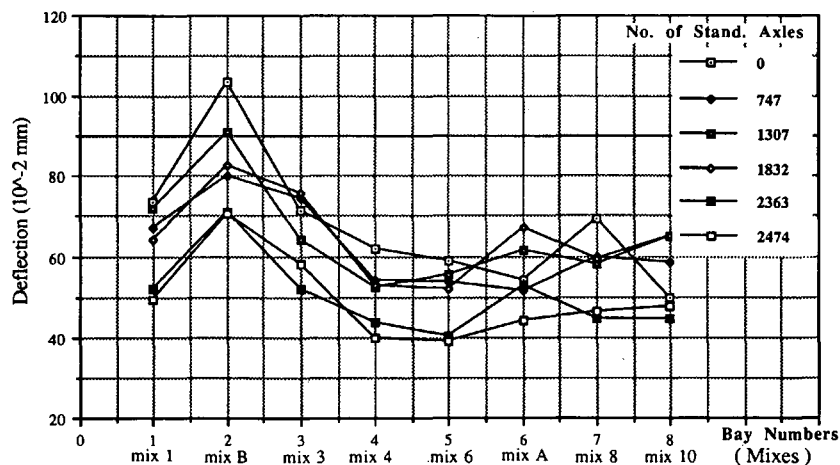


FIGURE 10 Deflection versus standard axle passed at Dargan Road in first month.



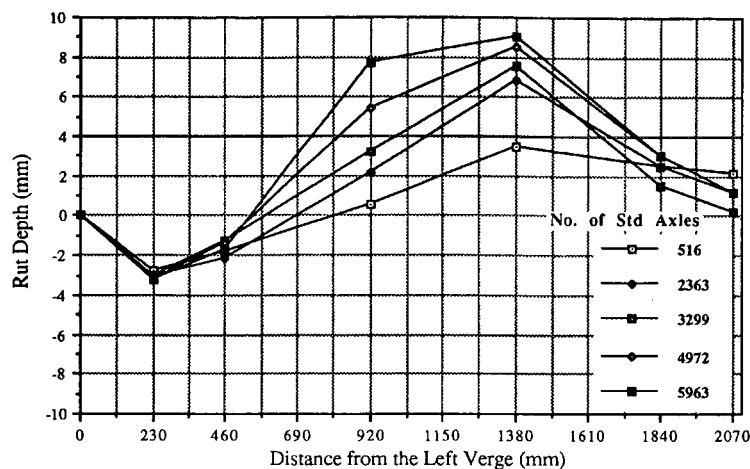


FIGURE 11 Rut depth versus standard axles passed for Bay 5 (Mix 6).

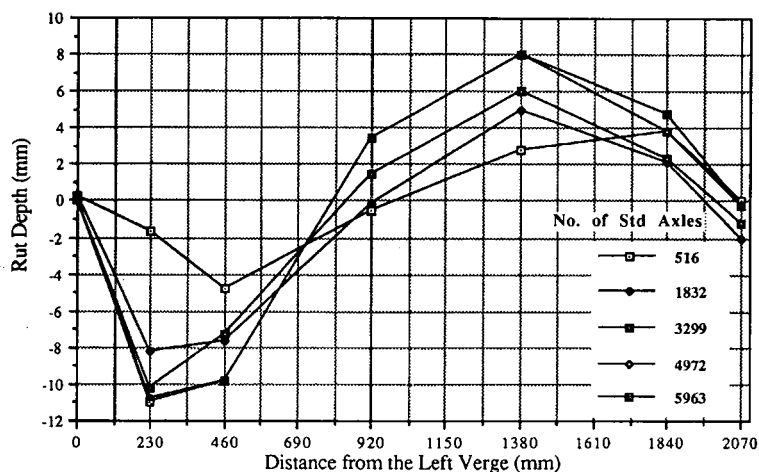


FIGURE 12 Rut depth versus standard axles passed for Bay 6 (Mix A).

the laboratory (Mixes 8 and 10 showed higher plastic strain than the other mixes).

## DISCUSSION OF RESULTS

The above findings showed that the greater the percentage of material retained on a 5-mm sieve, the higher the stiffness. Whereas the open-graded mixes showed less resistance to permanent deformation, the well-graded mixes with a percentage of effective fines more than 50 percent showed less resistance to permanent deformation. It can be seen in Figure 3 that Mixes 3, 6, and 10 showed a greater stiffness than the other mixes tested, and mixes 3 and 6 also showed greater resistance to permanent deformation (Figure 7).

Similar trends were observed on the full-scale testing strip. Mixes 3, 4, 6, and 10 showed lesser deflection, confirming that they had a higher elastic stiffness. The rut depths for mixes on the finer side of the envelope (Mixes 1, 3, 4, and 6, with high  $C_u$ ) were less than about half of those for the

mixes on the coarser side of the envelope (Mixes 8 and 10, with low  $C_u$ ). This was also confirmed by the trends obtained for the plastic strain for Mixes 8 and 10 in the repeated load triaxial laboratory tests; that is, they showed a higher permanent deformation as compared with Mixes 1, 3, 4, and 6. It can also be concluded that permanent deformation under repeated loading provides a more definitive evaluation of unbound granular materials than do resilient modulus and shear strength.

## CONCLUSIONS

The following may be concluded from the laboratory tests:

1. The elastic stiffness increases from the finer to the coarser end of the envelope.
2. The resilient volumetric and shear strains also implied a similar trend, that is, the resistance to shear and volumetric

strains increases from the finer to the coarser end of the proposed grading envelope.

3. The resistance to permanent deformation was less for more open-graded mixes compared with well-graded ones.

4. Shear strength increases from the finer to the coarser end of the envelope.

5. The permeability for the base, subbase, and capping layers for material used for road construction may be assessed with the help of the equation proposed in the section on permeability testing.

The following may be concluded from the test strip:

1. The material that had more effective fines showed a higher deflection, and as the effective fines content decreased, the deflection also decreased up to a certain value, after which a further reduction in effective fines resulted in a higher deflection. Thus, there was an optimum effective fines content for minimum deflection and rut.

2. Materials with a  $C_u$  from 25 to 40 and having an effective fines content from 27 to 44 percent showed low values for deflection and rut.

3. The elastic modulus was generally found to increase from the finer to the coarser end of the envelope.

4. The rut depth was found to be more than twice as great for the open-graded material as for the well-graded materials.

#### ACKNOWLEDGMENTS

This research was sponsored by the Roads Service of the Department of the Environment. The authors wish to acknowledge the help of the staff of the Department of Civil Engineering, University of Nottingham; the laboratory equipment provided by that department; and the sponsorship provided by the government of Pakistan.

#### REFERENCES

1. P. Shaw. *Stress-Strain Relationships for Granular Materials Under Repeated Loading*. Ph.D. thesis. University of Nottingham, 1980.
2. N. H. Thom. *Design of Road Foundations*. Ph.D. thesis. University of Nottingham, 1988.
3. M. R. Thompson and K. L. Smith. Repeated Load Triaxial Characterisation of Granular Bases. Presented at 69th Annual Meeting of the Transportation Research Board, Washington, D.C., 1990.
4. Roads Circular No. 19/87. Department of the Environment for NI Roads Service Headquarters, 1987.
5. K. E. Cooper, S. F. Brown, and G. R. Pooley. The Design of Aggregate Gradings for Asphalt Base Courses. *Proc., Association of Asphalt Paving Technologists, Technical Session*, San Antonio, Tex., 1985.
6. J. R. Boyce. *The Behaviour of Granular Material Under Repeated Loading*. Ph.D. thesis. University of Nottingham, 1976.
7. N. W. Lister and R. Jones. The Behaviour of Flexible Pavements Under Moving Wheel Loads. *Proc., 2nd International Conference on the Structural Design of Asphalt Pavements*, Ann Arbor, Mich., 1967.
8. J. W. Pappin. *Characteristics of a Granular Material for Pavement Analysis*. Ph.D. thesis. University of Nottingham, 1979.
9. J. R. Morgan. The Response of Granular Materials to Repeated Loading. *Proc., 3rd ARRB Conference*, 1966.
10. M. A. Kamal, O. T. Farouki, D. A. B. Hughes, and A. A. Sha'at. Influence of Grading on the Permeability and Performance of Subbase Materials. *The International Journal of Construction Maintenance and Repair*, Vol. 5, No. 6, Nov./Dec., 1991.
11. A Permeameter for Road Drainage Layers. Department of Transport Highways and Traffic, Departmental advice note HA 41/90, 1990.
12. E. G. Kleyn. *The Use of Dynamic Cone Penetrometer*. Report 12/74. Transvaal Roads Dept. Pretoria, South Africa, 1975.
13. M. A. Kamal. Behaviour of Granular Materials used in Flexible Pavements. 2nd Progress Report. Department of Environment, Northern Ireland, 1991.
14. Pavement Evaluation Program EVERCALC, Version 2.0., Washington State Transportation Center, 1988.
15. *Special Report 73: The AASHO Road Test*. HRB, National Research Council, Washington, D.C., 1962.

---

*Publication of this paper sponsored by Committee on Soil and Rock Properties.*